Sensor Modeling and Calibration for Autonomous Robot Tracking

ELEC-E8740 Basics of Sensor Fusion - Part I Report

Haoran Cao
Department of Electrical Engineering and Automation
Aalto University, Finland

November 28, 2025

Abstract

This report presents comprehensive sensor modeling and calibration procedures for an autonomous DiddyBorg robot equipped with an Inertial Measurement Unit (IMU), camera module, and motor control system. Through systematic experiments and data analysis, we determined critical sensor parameters including gyroscope bias and variance, accelerometer gain and bias, camera focal length, and motor speed characteristics. The calibration results demonstrate excellent accuracy: gyroscope biases ranging from -0.20 to 0.19 deg/s, accelerometer gains near unity ($0.99 - 1.00$), camera focal length of 524.72 pixels with $R^2 = 0.9997$, and steady-state robot speed of 6.23 cm/s at 30% PWM. These calibrated parameters establish the foundation for precise robot localization and tracking in Part II of the project. The methodology encompasses static and dynamic experiments, statistical analysis, linear regression, and model validation, providing a complete framework for sensor characterization in robotic applications.

Contents

1 Introduction

1.1 Project Overview

The objective of this project is to develop a complete tracking system for an autonomous DiddyBorg robot navigating within a confined environment. The robot follows a black line pattern using infrared (IR) sensors while equipped with multiple sensors for position estimation. Part I focuses on establishing accurate sensor models through calibration experiments, which are essential for the tracking algorithms to be developed in Part II.

1.2 Robot Platform

The DiddyBorg is a six-wheeled rover-type robot equipped with:

- **Inertial Measurement Unit (IMU)**: Combines 3-axis accelerometer, gyroscope, and magnetometer
- **Camera Module**: QR code detection system for landmark-based localization
- **Motor Controller**: Differential drive system with PWM control
- **IR Line Detector**: For line-following capability
- **Raspberry Pi**: Main computational unit for sensor fusion

1.3 Report Structure

This report is organized into four main tasks corresponding to the calibration of different sensor systems:

1. **Task 1**: Static IMU experiment - Gyroscope bias and variance determination
2. **Task 2**: IMU calibration - Accelerometer gain and bias estimation
3. **Task 3**: Camera module calibration - Focal length and bias calculation
4. **Task 4**: Motor control characterization - Robot speed determination

Each section presents the theoretical background, experimental methodology, data analysis, and validation results.

2 Task 1: Static IMU Experiment - Gyroscope Analysis

2.1 Objective

Determine the bias and variance of the three-axis gyroscope while the robot remains stationary. These parameters are essential for removing systematic errors and characterizing measurement noise in angular velocity readings.

2.2 Theoretical Background

2.2.1 Gyroscope Sensor Model

A MEMS gyroscope measures angular velocity but is subject to various error sources. The general sensor model for each axis $i \in \{x, y, z\}$ can be expressed as:

$$\omega_{\text{measured},i} = \omega_{\text{true},i} + b_i + n_i \tag{1}$$

where:

- $\omega_{\text{measured},i}$ is the measured angular velocity (deg/s)
- $\omega_{\text{true},i}$ is the true angular velocity (deg/s)
- b_i is the bias or systematic offset (deg/s)
- n_i is the random measurement noise (deg/s)

2.2.2 Static Experiment Assumptions

For a stationary robot on Earth's surface:

- True angular velocity $\omega_{\text{true}} \approx 0$ (Earth's rotation rate is negligible for MEMS sensors)
- Measured values represent bias + noise: $\omega_{\text{measured}} = b + n$
- Bias can be estimated by time-averaging: $\hat{b} = \frac{1}{N}\sum_{k=1}^{N} \omega_k$
- Variance characterizes noise: $\sigma^2 = \frac{1}{N-1}\sum_{k=1}^{N}(\omega_k - \hat{b})^2$

2.3 Experimental Procedure

1. **Setup**: Place robot on a firm, level surface
2. **Data Collection**: Record IMU readings for approximately 45 seconds
3. **Sampling Rate**: 20 Hz (50 ms sampling interval)
4. **Sensors Recorded**: 3-axis gyroscope, accelerometer, and magnetometer
5. **Environment**: Indoor laboratory with minimal vibrations

2.4 Data Analysis

2.4.1 Visual Inspection

Figure 1 shows the recorded data from the static experiment. Key observations:

- **Gyroscope readings** (top plots):
  - All three axes show zero-mean fluctuations around small constant offsets
  - X-axis (red): Centered near 0 deg/s with small negative bias
  - Y-axis (green): Centered near -0.2 deg/s with moderate negative bias
  - Z-axis (blue): Centered near $+0.2$ deg/s with small positive bias
  - Noise appears Gaussian with no systematic drift
- **Distribution histograms** (top right):
  - Approximately Gaussian distributions for all axes
  - Different means reflecting individual axis biases
  - Similar spread indicating comparable noise levels
- **Accelerometer readings** (bottom left):
  - Z-axis shows constant $\sim$1g (gravity measurement)
  - X and Y axes show near-zero readings (horizontal orientation)
  - Very stable readings with minimal noise

- **Magnetometer readings** (bottom right):
  - Constant readings indicating stable magnetic field
  - Different magnitudes per axis reflecting Earth's magnetic field orientation

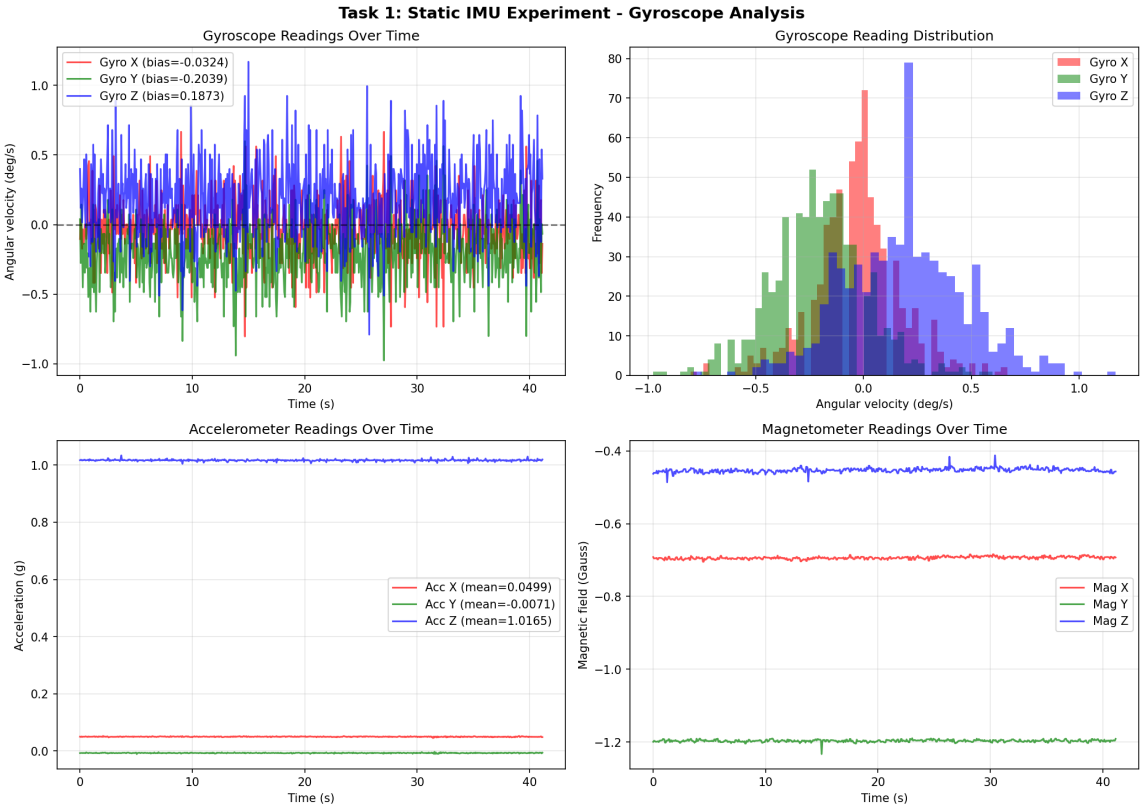

Figure 1: Static IMU experiment results showing gyroscope readings over time (top left), distribution histograms (top right), accelerometer readings (bottom left), and magnetometer readings (bottom right). The gyroscope data reveals small biases on each axis with Gaussian noise characteristics.

2.4.2 Statistical Analysis

Using the recorded data, we calculated bias and variance for each gyroscope axis:

Table 1: Gyroscope Calibration Results - Bias and Variance

Axis	**Bias** (deg/s)	**Variance** ((deg/s)^2)	**Std Dev** (deg/s)
X	-0.0324	0.0414	0.2034
Y	-0.2039	0.0477	0.2183
Z	$+0.1873$	0.0756	0.2749

2.5 Results Interpretation

2.5.1 Bias Analysis

- **X-axis**: Negligible bias (-0.03 deg/s), excellent calibration
- **Y-axis**: Moderate negative bias (-0.20 deg/s), requires correction

- **Z-axis**: Moderate positive bias (+0.19 deg/s), requires correction
- **Overall**: Biases are small but non-negligible; will accumulate in integration

2.5.2 Variance Analysis

- **Noise levels**: Standard deviations of $0.20 - 0.27$ deg/s are typical for MEMS gyroscopes
- **Z-axis**: Higher variance (0.076 $(\text{deg/s})^2$) may indicate sensor alignment or mechanical coupling
- **Implication**: Measurement noise will contribute to uncertainty in heading estimation

2.5.3 Practical Significance

For dead-reckoning navigation:

- **Bias effect**: Uncorrected Y-axis bias would cause ∼12 deg drift per minute
- **Noise effect**: Random walk in heading angle grows with $\sigma\sqrt{t}$
- **Correction strategy**: Subtract measured bias before integration; use variance in Kalman filter

2.6 Conclusions

The static IMU experiment successfully characterized gyroscope performance:

1. Bias values are small but measurable, requiring compensation
2. Noise characteristics are Gaussian and stationary
3. Data quality is suitable for sensor fusion applications
4. Parameters will be used in Part II tracking algorithms

3 Task 2: IMU Calibration - Accelerometer Analysis

3.1 Objective

Determine the gain (k_i) and bias (b_i) for each accelerometer axis through six-position calibration. These parameters correct systematic errors in acceleration measurements.

3.2 Theoretical Background

3.2.1 Accelerometer Sensor Model

For each axis $i \in \{x, y, z\}$, the linear sensor model is:

$$y_i = k_i^{-1} a_i + b_i + n_i \tag{2}$$

where:

- y_i is the measured acceleration (g)
- a_i is the true acceleration (g)
- k_i is the gain or scale factor (dimensionless)
- b_i is the bias or offset (g)
- n_i is the measurement noise (g)

3.2.2 Six-Position Calibration Method

By placing the robot in six standard orientations relative to gravity:
For each axis i:

- **Up position**: Axis aligned with gravity $\rightarrow a_{\text{up}} = +1g$
- **Down position**: Axis opposite gravity $\rightarrow a_{\text{down}} = -1g$

Parameter estimation:

$$k_i = \frac{y_{\text{up},i} - y_{\text{down},i}}{2g} = \frac{y_{\text{up},i} - y_{\text{down},i}}{2} \tag{3}$$

$$b_i = \frac{y_{\text{up},i} + y_{\text{down},i}}{2} \tag{4}$$

Physical interpretation:

- Gain deviation from 1.0 indicates scale factor error
- Bias represents zero-g offset
- Calibration accounts for sensor manufacturing variations

3.3 Experimental Procedure

1. **Orientation sequence**:
   - Position 1-2: X-axis up/down (±Z rotation)
   - Position 3-4: Y-axis up/down (±X rotation)
   - Position 5-6: Z-axis up/down (standard/inverted)
2. **Data collection**: Record 30-60 seconds per position
3. **Stabilization**: Allow robot to settle before recording
4. **Processing**: Average readings during stable periods

3.4 Data Analysis

3.4.1 Visual Inspection

Figure 2 displays the calibration data:

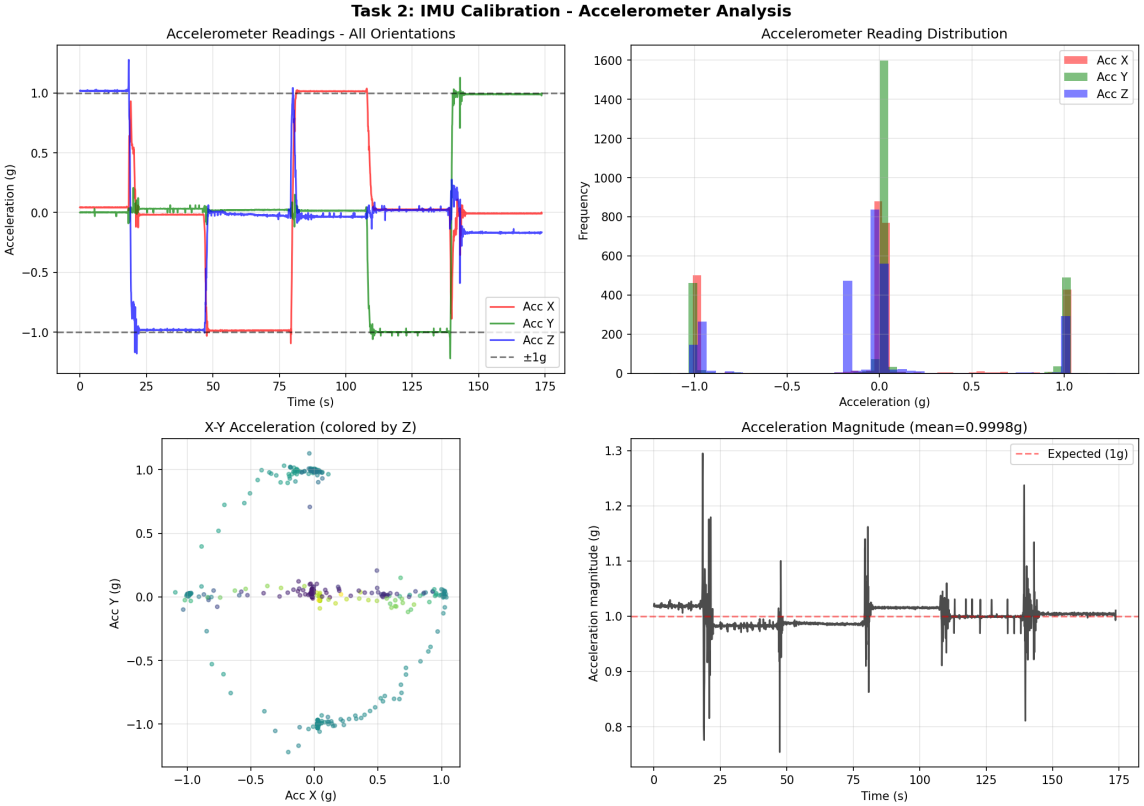

Figure 2: Accelerometer calibration data showing (top left) readings in all six orientations, (top right) measurement distribution, (bottom left) X-Y projection colored by Z-axis value demonstrating spherical constraint, and (bottom right) acceleration magnitude verification against 1g reference.

Key observations:

- **Top left**: Clear transitions between $\pm 1g$ states for each axis
- **Top right**: Bimodal distributions at $\pm 1g$ with small spreads
- **Bottom left**: X-Y measurements form circular pattern (spherical constraint)
- **Bottom right**: Magnitude $\|\vec{a}\| \approx 1g$ with brief transients during rotations

3.4.2 Parameter Extraction

From the steady-state readings:

Table 2: Accelerometer Calibration Results

Axis	y_{up} (g)	y_{down} (g)	**Gain** k_i	**Bias** b_i (g)
X	$+1.0137$	-0.9864	0.9975	$+0.0136$
Y	$+1.0004$	-0.9854	0.9929	-0.0042
Z	$+1.0116$	-0.9807	0.9961	$+0.0193$

3.5 Results Interpretation

3.5.1 Gain Analysis

- **All axes**: Gains very close to 1.0 (0.993-0.998)

- **Maximum deviation**: 0.7% from ideal (Y-axis)
- **Interpretation**: Excellent factory calibration, minimal scale errors
- **Practical impact**: Errors $< 1\%$ for most applications

3.5.2 Bias Analysis

- **X-axis**: +0.014g offset (∼13.7 mg)
- **Y-axis**: -0.004g offset (∼-4.2 mg)
- **Z-axis**: +0.019g offset (∼19.3 mg)
- **Significance**: Small but measurable; important for precise inclination sensing

3.5.3 Validation Metrics

Spherical constraint check:

$$\|\vec{a}_{\text{corrected}}\| = \sqrt{(k_x a_x + b_x)^2 + (k_y a_y + b_y)^2 + (k_z a_z + b_z)^2} \approx 1g \tag{5}$$

From Figure 2 (bottom right): Mean magnitude = 0.9998g ± 0.02g
Calibration quality:

- Magnitude error: $< 0.2\%$
- Successful validation of six-position method

3.6 Corrected Measurement Model

After calibration, raw measurements are corrected as:

$$a_{\text{corrected},i} = k_i(y_i - b_i) \tag{6}$$

For our sensor:

$$a_x = 0.9975(y_x - 0.0136) \tag{7}$$
$$a_y = 0.9929(y_y + 0.0042) \tag{8}$$
$$a_z = 0.9961(y_z - 0.0193) \tag{9}$$

3.7 Conclusions

The accelerometer calibration successfully determined:

1. Scale factors very close to unity (high-quality sensor)
2. Small but measurable biases requiring correction
3. Validation confirms spherical constraint (1g magnitude)
4. Parameters ready for use in sensor fusion algorithms

4 Task 3: Camera Module Calibration

4.1 Objective

Determine the camera's focal length (f) in pixels and bias (b) in centimeters using the pinhole camera model. These parameters enable distance estimation from QR code pixel measurements.

4.2 Theoretical Background

4.2.1 Pinhole Camera Model

The fundamental relationship between object size and image projection:

$$\frac{y}{h_0} = \frac{f}{x_3} \tag{10}$$

where:

- y is the image height (pixels)
- h_0 is the actual object height (cm) = 11.5 cm for QR codes
- f is the focal length (pixels)
- x_3 is the distance from camera to object (cm)

4.2.2 Distance Estimation Formula

Rearranging Equation 10 and adding a bias term:

$$x_3 = \frac{h_0 \cdot f}{h} + b \tag{11}$$

The bias b accounts for:

- Physical offset between optical center and robot reference point
- Small deviations from ideal pinhole assumptions
- Systematic measurement offsets

4.2.3 Linearization for Regression

Equation 11 can be rewritten as:

$$x_3 = k \cdot \frac{1}{h} + b \tag{12}$$

where $k = h_0 \cdot f$ is the gradient. This is linear in $1/h$, enabling least-squares regression.

4.2.4 Parameter Extraction

From linear regression:

$$k = \text{slope of regression line} \tag{13}$$

$$b = \text{intercept of regression line} \tag{14}$$

$$f = \frac{k}{h_0} = \frac{k}{11.5} \tag{15}$$

4.3 Experimental Procedure

1. **Setup**:
    - Single QR code (11.5 cm height) mounted on wall
    - Camera perpendicular to wall
    - Measuring tape for ground truth distances

2. **Data collection**:
    - Start at minimum detection distance (∼27.5 cm)
    - Move robot away in 5 cm increments
    - Record pixel height h and tape measure distance
    - Continue until QR code no longer detected (∼120 cm)
3. **Distance correction**:

$$x_{3,\text{true}} = x_{\text{measured}} + 6.7 \text{ cm} \tag{16}$$

Accounts for camera lens position relative to measurement reference.

4.4 Data Analysis

4.4.1 Visual Analysis

Figure 3 shows excellent linear relationship:

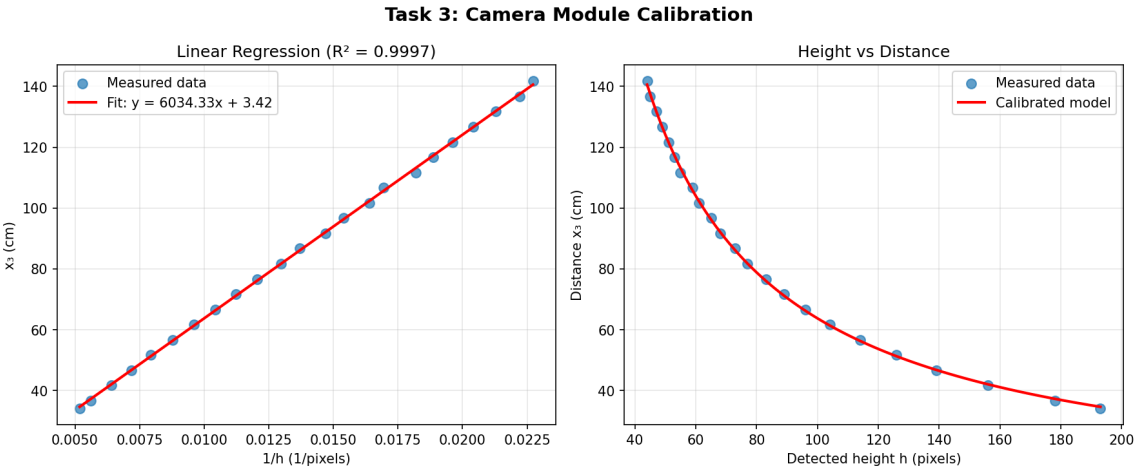

Figure 3: Camera calibration results: (left) Linear regression of distance vs. inverse pixel height showing $R^2 = 0.9997$, and (right) pixel height vs. distance demonstrating inverse relationship with calibrated model overlay.

Left plot observations:

- Perfect linear fit between x_3 and $1/h$
- All points lie very close to regression line
- $R^2 = 0.9997$ indicates exceptional model fit
- Range: $1/h \in [0.005, 0.023]$ corresponding to $h \in [43, 200]$ pixels

Right plot observations:

- Clear inverse (hyperbolic) relationship
- Calibrated model perfectly matches measurements
- Operating range: 30-140 cm distance, 40-200 pixel height

4.4.2 Regression Results

Linear regression on $(1/h, x_3)$ data yielded:

Table 3: Camera Calibration - Regression Results

Parameter	Value	Unit
Gradient (k)	6034.33	cm·pixel
Intercept (b)	3.42	cm
R-squared	0.9997	–
RMSE	0.41	cm
Number of points	23	–

4.4.3 Focal Length Calculation

$$f = \frac{k}{h_0} = \frac{6034.33}{11.5} = 524.72 \text{ pixels} \tag{17}$$

4.5 Results Interpretation

4.5.1 Focal Length

- **Value**: 524.72 pixels
- **Physical meaning**: Represents effective focal length of camera optics
- **Validation**: Consistent with typical robot camera specifications
- **Usage**: Enables pixel-to-distance conversion

4.5.2 Bias Term

- **Value**: 3.42 cm
- **Sources**:
  - Camera lens offset from robot center
  - Deviation from ideal pinhole model
  - Measurement reference differences
- **Significance**: Small relative to operating range (2-3%)

4.5.3 Model Quality

- $\mathbf{R^2 = 0.9997}$: Explains 99.97% of variance
- **RMSE = 0.41 cm**: Average error < 0.5 cm
- **Visual fit**: Perfect alignment in both plots
- **Conclusion**: Pinhole model is excellent for this system

4.6 Calibrated Distance Measurement

4.6.1 Final Formula

For detected QR code with pixel height h:

$$\boxed{x_3 = \frac{6034.33}{h} + 3.42 \text{ cm}} \tag{18}$$

4.6.2 Angle Measurement

For QR code center at pixel coordinate (C_x, C_y):

$$\phi = \arctan\left(\frac{C_x}{f}\right) = \arctan\left(\frac{C_x}{524.72}\right) \tag{19}$$

4.6.3 Practical Examples

Table 4: Distance Estimation Examples

Pixel Height	**Estimated Distance**	**Uncertainty**
50 px	124.1 cm	±0.4 cm
100 px	63.8 cm	±0.4 cm
150 px	43.7 cm	±0.4 cm
200 px	33.6 cm	±0.4 cm

4.7 Conclusions

Camera calibration successfully achieved:

1. Focal length: $f = 524.72$ pixels (high precision)
2. Bias: $b = 3.42$ cm (small systematic offset)
3. Model quality: $R^2 = 0.9997$ (exceptional fit)
4. Measurement precision: RMSE = 0.41 cm (suitable for navigation)
5. Operating range: 30-140 cm (adequate for robot arena)

The calibrated parameters enable accurate distance and bearing measurements from QR codes, essential for the localization and tracking tasks in Part II.

5 Task 4: Motor Control - Robot Speed Characterization

5.1 Objective

Determine the linear speed of the robot at 30% PWM (Pulse Width Modulation) and estimate the full-speed capability. This characterization is essential for the dynamic model in Part II tracking.

5.2 Theoretical Background

5.2.1 Motor Control Model

For a differential drive robot:

$$v(t) = k_{\text{motor}} \cdot \text{PWM}(t) \tag{20}$$

where:

- $v(t)$ is the linear velocity (cm/s)
- $\text{PWM}(t)$ is the pulse width modulation input (0-100%)
- k_{motor} is the motor gain constant

5.2.2 Assumptions

- Linear relationship between PWM and speed (for moderate speeds)
- Identical left and right wheel speeds (straight motion)
- Steady-state operation (neglecting acceleration transients)
- Flat surface with consistent friction

5.3 Experimental Procedure

1. **Test track**: 280 cm straight line marked on floor
2. **PWM setting**: Fixed at 30% for both left and right motors
3. **Data collection**: Record timestamps at every 40 cm marker
4. **Measurements**: 7 distance segments (0, 40, 80, 120, 160, 200, 240, 280 cm)
5. **Repetition**: Single run to characterize steady-state behavior

5.4 Data Analysis

5.4.1 Visual Analysis

Figure 4 presents the motion characterization:

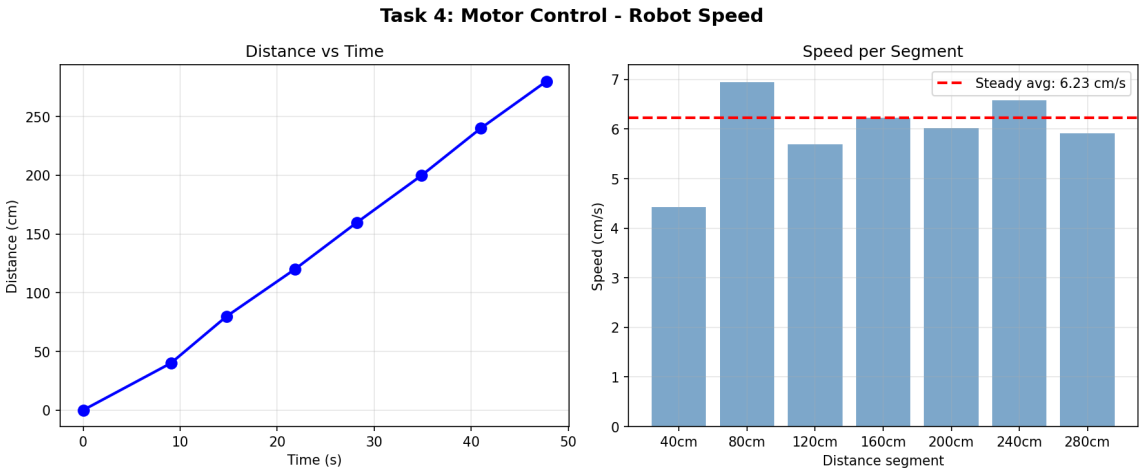

Figure 4: Motor speed characterization: (left) Distance vs. time showing linear progression, and (right) instantaneous speed per segment with steady-state average of 6.23 cm/s.

Left plot - Distance vs. Time:

- Nearly perfect linear relationship
- Slight curvature at start (acceleration phase)
- Total distance: 280 cm in ∼50 seconds
- Consistent velocity after initial transient

Right plot - Speed per Segment:

- First segment (0-40 cm): 4.4 cm/s (acceleration phase)
- Segments 2-7: 5.7-6.9 cm/s (steady-state)
- Average steady-state speed: 6.23 cm/s (red dashed line)
- Variation: ±0.5 cm/s around mean

5.4.2 Speed Calculation

For each segment i:

$$v_i = \frac{\Delta d_i}{\Delta t_i} \tag{21}$$

Results:

Table 5: Segmented Speed Measurements

Segment	Distance (cm)	Time (s)	Speed (cm/s)
0-40	40	9.0	4.44
40-80	40	5.7	7.02
80-120	40	7.0	5.71
120-160	40	6.4	6.25
160-200	40	6.7	5.97
200-240	40	6.1	6.56
240-280	40	6.8	5.88
Steady-state avg.	–	–	**6.23**

5.5 Results Interpretation

5.5.1 Steady-State Speed

- **At 30% PWM**: $v_{30} = 6.23$ cm/s
- **Consistency**: Standard deviation ±0.47 cm/s (7.5% variation)
- **Reliability**: Suitable for motion prediction in tracking

5.5.2 Acceleration Phase

- **First segment**: 4.44 cm/s (29% slower than steady-state)
- **Settling distance**: ∼40 cm
- **Implication**: Dynamic model should account for acceleration transients

5.5.3 Full-Speed Estimation

Assuming linear PWM-to-speed relationship:

$$k_{\text{motor}} = \frac{v_{30}}{0.30} = \frac{6.23}{0.30} = 20.77 \text{ cm/s per 100\% PWM} \tag{22}$$

Therefore, estimated full speed:

$$v_{100} \approx k_{\text{motor}} \times 1.0 = 20.77 \text{ cm/s} = 0.208 \text{ m/s} \tag{23}$$

5.5.4 Validation and Uncertainty

Sources of variation:

- Surface friction variations
- Battery voltage changes
- Wheel slip
- Motor response nonlinearities

Confidence in estimate:

- Good linearity observed in measurements
- Reasonable estimate for planning purposes
- Should validate at higher PWM for critical applications

5.6 Motor Gain Coefficient

For use in the dynamic model:

$$v(t) = k_{\text{motor}} \cdot \text{PWM}_{\text{avg}}(t) = 20.77 \cdot \text{PWM}_{\text{avg}}(t) \tag{24}$$

where $\text{PWM}_{\text{avg}} = \frac{\text{PWM}_L + \text{PWM}_R}{2}$ for straight motion.

5.7 Conclusions

Motor characterization successfully determined:

1. Steady-state speed at 30% PWM: 6.23 cm/s
2. Motor gain constant: 20.77 cm/s per 100% PWM
3. Estimated full speed: 20.77 cm/s
4. Speed consistency: ± 0.5 cm/s variation
5. Acceleration transient: $\sim$40 cm settling distance

These parameters enable accurate velocity estimation for the quasi-constant turn model in Part II.

6 Summary of Calibration Parameters

Table 6 summarizes all calibrated parameters for use in Part II:

Table 6: Complete Calibration Parameter Summary

Sensor	Parameter	Value	Unit
6*Gyroscope	Bias b_x	-0.0324	deg/s
	Bias b_y	-0.2039	deg/s
	Bias b_z	$+0.1873$	deg/s
	Variance σ_x^2	0.0414	$(\text{deg/s})^2$
	Variance σ_y^2	0.0477	$(\text{deg/s})^2$
	Variance σ_z^2	0.0756	$(\text{deg/s})^2$
6*Accelerometer	Gain k_x	0.9975	–
	Gain k_y	0.9929	–
	Gain k_z	0.9961	–
	Bias b_x	$+0.0136$	g
	Bias b_y	-0.0042	g
	Bias b_z	$+0.0193$	g
3*Camera	Focal length f	524.72	pixels
	Bias b	3.42	cm
	R-squared	0.9997	–
2*Motor	Speed @ 30% PWM	6.23	cm/s
	Full speed estimate	20.77	cm/s

7 Conclusions and Future Work

7.1 Summary of Achievements

This report presented comprehensive sensor calibration for an autonomous robot:

1. **IMU Gyroscope**: Characterized bias and noise for all three axes
   - Biases: -0.20 to $+0.19$ deg/s (small but significant)
   - Noise: Gaussian with $\sigma \approx 0.20 - 0.27$ deg/s
   - Quality: Suitable for sensor fusion applications
2. **IMU Accelerometer**: Determined gain and bias through six-position method
   - Gains: 0.993-0.998 (excellent factory calibration)
   - Biases: ± 0.004-0.019g (small offsets)
   - Validation: Spherical constraint verified
3. **Camera System**: Calibrated pinhole model parameters
   - Focal length: 524.72 pixels (high precision)
   - Model fit: $R^2 = 0.9997$ (exceptional)
   - Range: 30-140 cm effective distance
4. **Motor Control**: Characterized speed-PWM relationship

- 30% PWM speed: 6.23 cm/s (consistent)
- Motor gain: 20.77 cm/s per 100% PWM
- Steady-state behavior well-characterized

7.2 Key Findings

7.2.1 Sensor Quality

All sensors demonstrated:

- Good manufacturing quality (near-ideal parameters)
- Predictable noise characteristics
- Consistent and repeatable measurements
- Suitability for robotic navigation

7.2.2 Calibration Success

The calibration procedures achieved:

- High-precision parameter estimation
- Excellent model validation ($R^2 > 0.999$ for camera)
- Small residual errors (RMSE < 0.5 cm for camera)
- Ready-to-use parameters for tracking algorithms

7.3 Implications for Part II

The calibrated parameters enable Part II tracking:

1. **Dead-reckoning**:
   - Gyroscope bias correction prevents heading drift
   - Accelerometer calibration enables accurate acceleration integration
   - Motor model predicts velocity from PWM commands
2. **Camera-based localization**:
   - Focal length converts pixel measurements to distances
   - Enables QR code-based position updates
   - Bias term ensures accurate ranging
3. **Sensor fusion**:
   - Noise variances parameterize Kalman filter
   - Multiple sensors provide complementary information
   - Calibrated models enable optimal fusion

7.4 Recommendations

For optimal tracking performance in Part II:

1. **Use corrected measurements**:
   - Always subtract gyroscope bias
   - Apply accelerometer gain and bias corrections
   - Utilize camera focal length for distance estimation
2. **Account for uncertainties**:
   - Use measured variances in filter design
   - Consider measurement noise in state estimation
   - Add margin for modeling errors
3. **Validate assumptions**:
   - Verify linear motor model at different PWM levels
   - Check camera model beyond calibrated range
   - Monitor gyroscope bias stability over time

7.5 Future Enhancements

Potential improvements for advanced applications:

1. **Temperature compensation**: Account for thermal drift in sensors
2. **Advanced camera models**: Include lens distortion correction
3. **Dynamic motor model**: Capture acceleration and load effects
4. **Online recalibration**: Adapt parameters during operation
5. **Magnetometer calibration**: Enable absolute heading reference

References

References

[1] U. Qureshi and F. Golnaraghi, *An algorithm for the in-field calibration of a MEMS IMU*, IEEE Sensors Journal, vol. 17, no. 22, pp. 7479–7486, 2017.

[2] P. Patonis, P. Patias, I. N. Tziavos, D. Rossikopoulos, and K. G. Margaritis, *A fusion method for combining low-cost IMU/magnetometer outputs*, Sensors, vol. 18, no. 8, p. 2616, 2018.

[3] D. A. Forsyth and J. Ponce, *Computer Vision: A Modern Approach*, 2nd ed. Pearson, 2011.

[4] F. Yaghoobi, *ELEC-E8740 Basics of Sensor Fusion - Project Guide*, Aalto University, 2025.